Journal of Anatomy

J. Anat. (2018) **232**, pp15–25 doi: 10.1111/joa.12718

A guide for effective anatomical vascularization studies: useful *ex vivo* methods for both CT and MRI imaging before dissection

Yohann Renard,[1,2,3] Gabriela Hossu,[3,4] Bailiang Chen,[3,4] Marine Krebs,[1] Marc Labrousse[2] and Manuela Perez[1,3]

[1]*Department of Anatomy, Faculty of Medicine and University Hospital, University of Lorraine, Nancy, France*
[2]*Department of Anatomy, Faculty of Medicine and University Hospital, University of Reims Champagne-Ardenne, Reims, France*
[3]*IADI, INSERM U947, University of Lorraine, Nancy, France*
[4]*INSERM CIT1433, CIC-IT, University Hospital of Nancy, Nancy, France*

Abstract

The objective of this study was to develop a simple and useful injection protocol for imaging cadaveric vascularization and dissection. Mixtures of contrast agent and cast product should provide adequate contrast for two types of *ex vivo* imaging (MRI and CT) and should harden to allow gross dissection of the injected structures. We tested the most popular contrast agents and cast products, and selected the optimal mixture composition based on their availability and ease of use. All mixtures were first tested *in vitro* to adjust dilution parameters of each contrast agent and to fine-tune MR imaging acquisition sequences. Mixtures were then injected in 24 pig livers and one human pancreas for MR and computed tomography (CT) imaging before anatomical dissection. Colorized latex, gadobutrol and barite mixture met the above objective. Mixtures composed of copper sulfate ($CuSO_4$) gadoxetic acid (for MRI) and iodine (for CT) gave an inhomogeneous signal or extravasation of the contrast agent. Agar did not harden sufficiently for gross dissection but appears useful for CT and magnetic resonance imaging (MRI) studies without dissection. Silicone was very hard to inject but achieved the goals of the study. Resin is particularly difficult to use but could replace latex as an alternative for corrosion instead of dissection. This injection protocol allows CT and MRI images to be obtained of cadaveric vascularization and anatomical casts in the same anatomic specimen. Post-imaging processing software allow easy 3D reconstruction of complex anatomical structures using this technique. Applications are numerous, e.g. surgical training, teaching methods, postmortem anatomic studies, pathologic studies, and forensic diagnoses.

Key words: blood vessels; cadaver; corrosion casting; dissection; embalming; intra-arterial; teaching; vascular surgical procedures.

Introduction

The first knowledge of vascular anatomy was obtained from dissections on animals by Herophilus (ca. 340 BC) and then Galen (ca. 129–200 AD). Vesalius (1543) established the basis of human vessel anatomy from extensive cadaveric dissections (Bergeron et al. 2006). Injection of dyes to delineate vessels during dissection was first used by Jean Riolan (1580–1657). Many dyes were used afterwards for the study of vessels anatomy such as saffron, carmine, Prussian blue, India ink, and silver nitrate (Fye, 1984). During the 17th and 18th centuries, Lower, Swammerdam, de Graaf and Ruysch were the first anatomists to use fluid vector that solidifies (wax) direct vascular injections to facilitate the dissections (Fye, 1984; Bergeron et al. 2006; Grabherr et al. 2007). Discovery of X-ray in 1895 by Röntgen allowed injection of radiopaque markers. Heinrich Hildebrand published a stereoscopic atlas of roentgenograms of the human arterial system in 1901 (Fye, 1984). Since these scientific insights, particularly during the first half of the 20th century, numerous contrast agents and injection techniques have been introduced (Grabherr et al. 2007, 2015).

Correspondence
Yohann Renard, Department of Anatomy, Faculty of Medicine and University Hospital, University of Reims Champagne-Ardenne, Rue Cognacq-Jay, 51092 Reims Cedex, France. T: +33 3 26787094;
E: yrenard@chu-reims.fr

These authors contributed equally to this work.

Accepted for publication *5 September 2017*
Article published online *11 October 2017*

© 2017 Anatomical Society

Precise knowledge of vascular anatomy is still necessary, especially for planning surgical strategies (Zhao et al. 2002) such as perforator flap reconstructions (Kamali et al. 2016) and liver resection (Xiao et al. 2016). Currently, magnetic resonance imaging (MRI) and computed tomography (CT) are the accepted diagnostic tools in angiography, largely used in preoperative studies, but also for teaching methods, postmortem anatomic, pathologic, and forensic diagnoses, since colored fixated vessel system actually helps in pathological or forensic diagnosis (Grabherr et al. 2007; Bruguier et al. 2015; Blery et al. 2016). These rapidly developing techniques have allowed high-quality angiograms to be obtained (Zhang et al. 2007; Pabst et al. 2014; Saran et al. 2014) as well as creating virtual reality applications and 3D visualizations in surgery education (Lange et al. 2000; Friedl et al. 2002; Kamali et al. 2016; Pujol et al. 2016).

Ex vivo studies provide excellent models to study vascular trees and their variations (Rees & Taylor, 1986; Plaisant et al. 1998; Stokes et al. 1998; Friedl et al. 2002; Zhao et al. 2002; Godat et al. 2004; Bergeron et al. 2006; Zhang et al. 2007; Ruder et al. 2014; Grabherr et al. 2015; Blery et al. 2016; Kingston et al. 2016; Xiao et al. 2016). *Ex vivo* anatomical studies allow the injection of a permanent mixture, including casting techniques (Bergeron et al. 2006; Grabherr et al. 2007). But in modern medical diagnostic angiography methods, the contrast agent must be harmless and has to remain liquid, as in the field of forensic diagnosis, because the contrast mixture must be able to be washed out without leaving any traces in the body. Unfortunately, due to the advantages of CT-/MR-angiography with excellent 3D-reconstruction software, historical contrasts agents are no longer used for *ex vivo* studies nowadays, in particular the barium sulfate, silicone and latex rubber techniques (Grabherr et al. 2007).

The ideal mixture for *ex vivo* anatomical studies should be radiopaque for CT imaging, but should also provide contrast enhancement in MRI since 3D reconstruction of MRI angiograms has revealed details and rendered possible measurements that have until now not been even contemplated (Plaisant et al. 1998; Grabherr et al. 2007, 2015). In addition, this mixture should be colored and should harden, for direct dissection to be measured, photographed and compared with imaging results (Plaisant et al. 1998; Godat et al. 2004).

The purpose of this study was to develop a colored, reliable, reproducible and easily obtainable mixture in an anatomy laboratory that can both produce a contrast on CT and MRI analysis, and become sufficiently hard to allow easy gross dissections after imaging.

Materials and methods

Contrast agent

Contrast agents were prepared in latex, silicone, agar or gelatin and resin (polyurethane) compounds with different colorants (acrylic paints or pigment). These substances are summarized in Table 1. Silicone, agar and gelatin solution required dilutions to obtain sufficient low viscosity for manual injection. The dilution ratios were assessed experimentally or based on the literature. All mixtures were systematically tinted using colorant, as already advised by the manufacturers (Table 1). Since we choose only non-toxic and safe contrast agent and solution, all mixtures were prepared in 50-mL clear conical Falcon® tubes (Dutsher®, Brumath, France) on the laboratory bench.

The agar solution was obtained using 12 g agar powder mixed with 1000 mL demineralized water. The agar powder was gradually added to the boiling water. Powder should simmer for about 5 min to allow it to jellify. This liquid will begin to become gel when temperature falls below 45 °C, so it has to be made up just before injection. As the mixture cooled down, colorant and contrast agent were incorporated gradually while being agitated to obtain a homogeneous suspension and to avoid air bubbles. Silicone rubber and polyurethane resin were also prepared just before injection since once the hardener was added, they solidified quickly.

For CT, we tested iodine, barium sulfate and aluminum as a contrast agent media. For MRI, we tested copper sulfate ($CuSO_4$), gadoxetic acid and gadobutrol. For both CT and MRI agent contrast preparations we tested different concentrations. These are summarized in Table 2.

Specimen preparation

First, *in vitro* acquisitions were performed using 15-mL clear conical Falcon® tubes (Dutsher®) immerged in water. Contrast agent and solutions tested are summarized in Table 2.

Second, *ex vivo* porcine experiments were carried out. Twenty-four fresh pig livers were injected *ex vivo* with different mixtures and dissected in our anatomy laboratory by a surgeon. The livers came from the Nancy School of Surgery, Lorraine University, France, and were removed after surgical training sessions. This educational activity was approved by the CELMEA (Comité d'Ethique Lorrain en

Table 1 Solutions tested.

Solution	Manufacturer	Potential dilution	Colorant
Latex	Esprit composite, Paris, France	No dilution	Acrylic paints
Silicone	Wilsor Kunstharsen, Biddinghuizen, the Netherlands	Dilution with specific solution provided by the manufacturer (35%)	Pigment
Agar or gelatin	123gelules, Capbreton, France	Dilution with water (12 g agar/1000 mL water)	Acrylic paints
Resin (polyurethane)	Esprit composite, Paris, France	No dilution	Pigment

© 2017 Anatomical Society

Table 2 Contrast agents tested.

Contrast objective	Contrast agent	Manufacturer	Marketed concentration	Concentrations tested
CT	Barium sulphate	Guerbet, Roissy CdG, France	100 mg/100 mL	10% and 20%
	Iodine	Iomeron, GE Healthcare, Velizy-Villacoublay, France	350 and 400 mg mL^{-1}	5, 10, 20 and 30 mg mL^{-1}
		Gastrografine, Bayer Healthcare, Lyon, France	370 mg mL^{-1}	
		Radioselectan urinaire, Bayer Healthcare, Lyon, France	370 mg mL^{-1}	
	Lugol's iodine (nutritional supplement)	Health Leads UK, Ceredigion	40 mg mL^{-1}	5, 10 and 20 mg mL^{-1}
	Aluminium	Powder	Powder	7, 14, 20 and 100 g L^{-1}
MRI	$CuSO_4$	Sigma-Aldrich, l'Isle D'Abeau Chesnes, France	Powder $\geq$ 99%	0.5, 1, 2, 3, 4 and 5 g L^{-1}
	Gadoxetic acid	Guerbet, Roissy CdG, France	0.5 mmol mL^{-1}	1, 2, 4 and 10 mL L^{-1}
	Gadobutrol	Bayer Healthcare, Lyon, France	1 mmol L^{-1}	1, 2, 3 and 4 mL L^{-1}

Table 3 MRI parameters used according to the type of acquisition.

Acquisition	Repetition time (TR), ms	Echo time (TE), ms	Number of excitation (NEX)	Matrix	Field of view, mm^2	Slice thickness, mm	Flip angle	Resolution, mm^3
In vitro	5.5–7.4	1.7–2	3–8	200 × 200–384 × 256	270 × 270–370 × 370	1.8–2.2 (gap: 0.9–1.5)	20° (silicone: 40°)	N/A
Ex vivo pig liver	8.8–9.1	3.8–4.1	8	384 × 256	300 × 300–380 × 380	2 (gap: 1)	20°	0.8 × 1.2 × 2 to 0.9 × 1.4 × 2
Ex vivo human pancreas	7.4	2.9	6	360 × 290	290 × 290	0.6 (gap: 0.3)	20°	0.6 × 1 × 0.6

Matière d'Expérimentation Animale, agreement number C54-547-5). If liver surgery was performed on the pig, the organ was not removed. During the procedure, attention was paid to the aspect of the liver pedicle, in particular the hepatic artery. different mixtures were injected through a 19-gauge catheter inserted into hepatic artery of pig livers. A suture was tied around the vessel (with the catheter in the lumen) to hold the catheter in place. Injections through the hepatic artery of pig livers were performed either in the anatomy laboratory (9 pig livers), either in the MRI suite (15 pig livers), using a 20-mL syringe (BD Medical®, Le Pont-de-Claix, France). The injection was done manually and very gradually, until the colored mixture was seen on the organ surface; 20–50 mL was sufficient systematically to fill the pig liver arterial tree.

Before MR and CT examinations, pig livers were kept at 12 °C and then scanned at room temperature.

Finally, imaging on a 76-year-old female cadaver with injected pancreas vessels was performed. The cadaver was donated to the Department of Anatomy, Faculty of Medicine and University Hospital, Lorraine University, for anatomical education and research. This cadaver was studied following all ethical rules of work on cadaver material in our institution. A blue mixture was injected manually through a catheter introduced into the portal vein. Once the mixture was visible in the supra- and infra-mesenteric veins, these latter were clamped. A red mixture was injected in the supra-mesenteric artery. The abdominal aorta was previously clamped above the celiac trunk, and below the origin of the supra-mesenteric artery. The injection was stopped when the red mixture filled the hepatic artery, the splenic artery and the right gastric artery. The dissection was done using a scalpel, small dissection forceps and scissors.

MR imaging

MR experiments were performed on a 3T MR scanner (Signa HDxt; GE Healthcare, Milwaukee, WI, USA) with an 8-channel surface phased-array coil (8US TORSOPA). A 3D Fast Spoiled Gradient Echo (FSPGR) sequence was used for all images with varying parameters depending on the specimen type and size. The parameters used for each type of image are summarized in Table 3.

CT imaging

All examinations were performed using a 256-slice multidetector CT scanner (Revolution, General Electric Healthcare, USA) with the helical mode. The following parameters were used: 1.0 mm collimation, 120 kV, 110 mA, pitch 2, slice thickness 0.62 mm, matrix 512 × 512 and a field of view of 275 × 275 mm^2.

© 2017 Anatomical Society

Image data analysis

All post-processing was conducted with the 3D maximum intensity projection technique using Object Research System (ORS) Visual software version 1.5 (Montreal, Canada).

Signal characteristics were obtained by manually drawing a circular region of interest (ROI) of similar size (diameter 9–10 mm). ROIs were placed over the tubes and the vessels lumen of the pig livers.

To evaluate the extent of the enhancement of different mixtures to the structure, a new concept, enhancement efficiency, is defined for this study, as an analogy to the enhancement ratio used in MR perfusion studies (Hylton, 2006). The enhancement efficiency (E) was defined by subtracting the mean intensity in the non-injected vessel ($\text{mean}(I_{\text{noninjected\_vessel}})$) or tube from the injected same structures (liver tissue for *ex vivo* porcine specimen and water tube for *in vitro* experiments, ($\text{mean}(I_{\text{injected\_tissue}})$) divided by the non-injected same structures$\text{mean}(I_{\text{injected_tissue}})(Eq.1)$. This parameter is expressed in percentage. We consider an enhancement efficiency of 80% and above as a sufficient enhancement.

$$E = \frac{\text{mean}\left(I_{\text{injected\_tissue}}\right) - \text{mean}\left(I_{\text{noninjected\_vessel}}\right)}{\text{mean}\left(I_{\text{noninjected\_tissue}}\right)} \times 100\% \qquad (1)$$

For CT, target attenuation of 250 Hounsfield Units (HU) within the lumen (Nikolaou et al. 2004a,b) was considered sufficient intraluminal contrast enhancement for correct visualization and 3D reconstruction.

Results

In vitro tests

MRI and CT signal characteristics for all mixture are summarized in Table 4.

Briefly, we first mixed latex with iodine or barite (for CT) and $CuSO_4$ or gadoxetic acid (for MRI), providing good and homogeneous contrast. Silicone or agar mixed with the same contrast agents showed similar results as the latex one. The best concentrations of contrast agents for adequate contrast were 3 or 4 g L^{-1} for $CuSO_4$, 10% for barite, 20 mg mL^{-1} for iodine and 4 mL L^{-1} for gadoxetic acid (see Table 4 for detailed contrast enhancement efficiencies and concentrations). It is necessary to emphasize that the MRI sequence should be performed with a higher flip angle of 40° when using silicone as compared with a 20° flip angle with latex or agar.

Although $CuSO_4$, gadoxetic acid (for MRI) and iodine (for CT) are simple to use and provide satisfactory contrast enhancement, the signal was not homogenous, either at CT or MRI. In fact the contrast was more intense in the base of these tubes, probably because gadoxetic acid, $CuSO_4$ and iodine (but not barite) may sediment slightly. We then tested gadobutrol, a non-ionic, macrocyclic gadolinium-based MRI contrast agent, mixed with only barite according to our CT results described below in this section, in agar, latex and silicone. Barite (10%) and gadobutrol (3 mL L^{-1}) provided sufficient CT and MRI contrast, respectively (Table 4). These contrast agents did not sediment in tubes.

In the end, we tested resin. When mixed with barite or iodine (for CT), but not with gadobutrol, the resin provided an emulsion polymerization reaction that could not be injected. The only CT contrast agents not providing any emulsion reaction were aluminum powder (7–20 g L^{-1}) (Pauwels et al. 2014) and Lugol's iodine (20 mg L^{-1}) (see Tables 2 and 3), but they did not provide sufficient contrast enhancements for *in vitro* tests.

To summarize, the best contrast agents according to our *in vitro* tests were barite at a concentration of 10% mixed with gadobutrol at a concentration of 3 mL L^{-1}. Iodine and $CuSO_4$ or gadoxetic acid were very simple to use but sedimented slightly *in vitro.* Concerning the solutions, latex, agar and silicone showed similar satisfactory results, whereas resin was unworkable.

Ex vivo results

Imaging results using latex mixed with $CuSO_4$ or gadoxetic acid (for MRI) and barite or iodine (for CT) are shown in Fig. 1. Despite very encouraging *in vitro* results, latex mixed with $CuSO_4$ did not provide any contrast in *ex vivo* studies, whatever MR sequences were tested. Gadoxetic acid provided good MRI contrast, but the reconstruction of an arterial tree was not possible because of contrast agent extravasation. We tried to inject the gadoxetic acid in the MRI suite to shorten the delay between the injection and the MRI imaging but this did not prevent gadoxetic acid extravasation. CT scan showed the same contrast agent extravasation with iodine (Fig. 1A,B) but barite provided excellent contrast (702.8 HU, Fig. 1C,D) with a precise arterial tree on 3D reconstruction (Fig. 1D).

We tested gadobutrol (3 mL L^{-1}) as a contrast agent mixed with latex for MRI, as it is known to remain longer in the blood vessels. Injections into pig liver hepatic artery were performed in the MRI suite just before imaging to prevent any extravasation during the acquisition. The mixture gadobutrol–latex provided satisfactory contrast (enhancement efficiency 89%), allowing correct 3D reconstruction of the arterial tree (Fig. 2A,B). The mixture latex–gadobutrol–barite also provided excellent results at CT (996.3 HU) (Fig. 2C).

We then investigated agar and silicone. Following our *in vitro* results, only gadobutrol (3 mL L^{-1}) mixed with barite (10%), as contrast agent for MRI and CT, were used. Injections were always performed in the MRI suite just before imaging. The agar–gadobutrol–barite mixture provided adequate contrast, both at MRI (enhancement efficiency 150%) and CT (451.3 HU), but this mixture could not reach the distal ends of the arterial branches, probably because the agar cooled down too fast (Fig. 3A,C). The mixture silicone–gadobutrol–barite provided satisfactory contrast, both at MRI (enhancement efficiency 93%) and CT (510.5 HU), allowing nice 3D reconstructions of the arterial trees (Fig. 3D,F).

© 2017 Anatomical Society

© 2017 Anatomical Society

Table 4 MRI and CT signal characteristics for all *in vitro* tests.

Latex	Conc. of $CuSO_4$	Latex alone	5 g L^{-1}	4 g L^{-1}	3 g L^{-1}	2 g L^{-1}	1 g L^{-1}	0.5 g L^{-1}	
$CuSO_4$ (MRI)	Enhancement efficiency	−55%	38%	61%	78%	58%	−47%	−58%	
Iodine (CT)	Conc. of iodine	10 mg mL^{-1}	20 mg mL^{-1}						
	Signal attenuation (HU)	177	256						
Latex	Conc. of $CuSO_4$	Latex alone	5 g L^{-1}	4 g L^{-1}	3 g L^{-1}	2 g L^{-1}	1 g L^{-1}	0.5 g L^{-1}	
$CuSO_4$ (MRI)	Enhancement efficiency	−52%	135%	116%	160%	105%	−19%	−21%	
Barite (CT)	Conc. of barite	10%	20%						
	Signal attenuation (HU)	1170	1890						
Latex	Conc. of GA	10 mL L^{-1}	4 mL L^{-1}	2 mL L^{-1}	1 mL L^{-1}				
GA (MRI)	Enhancement efficiency	815%	973%	673%	594%				
Iodine or barite (CT)	Conc. of barite or iodine	10% (B)	20% (B)	10 mg mL^{-1} (Io)	20 mg mL^{-1} (Io)				
	Signal attenuation (HU)	1111	2190	−56	300				
Silicone $CuSO_4$ or	Conc. of $CuSO_4$ or GA	10 mL L^{-1} (GA)	4 mL L^{-1} (GA)	2 mL L^{-1} (GA)	1 mL L^{-1} (GA)	10 g L^{-1} ($CuSO_4$)	5 g L^{-1} ($CuSO_4$)	1 g L^{-1} ($CuSO_4$)	0.5 g L^{-1} ($CuSO_4$)
GA (MRI)	Enhancement efficiency	230%	512%	886%	1247%	610%	323%	180%	493%
Iodine or barite (CT)	Conc. of barite or iodine	10% (B)	20% (B)	10 mg m^{-1}L (Io)	20 mg mL^{-1} (Io)				
	Signal attenuation (HU)	1023	1416	450	720				
Agar $CuSO_4$ or	Conc. of $CuSO_4$ or GA	4 mL L^{-1} (GA)	2 mL L^{-1} (GA)	1 mL L^{-1} (GA)	3 g L^{-1} ($CuSO_4$)	4 g L^{-1} ($CuSO_4$)			
GA (MRI)	Enhancement efficiency	536%	388%	237%	143%	155%			
Iodine or barite (CT)	Conc. of barite or iodine	10% (B)	20% (B)	10 mg mL^{-1} (Io)	20 mg mL^{-1} (Io)	30 mg mL^{-1} (Io)			
	Signal attenuation (HU)	364.4	723.8	188	422.1	569.2			
Agar or silicone or latex	Conc. of gadobutrol	4 mL L^{-1} (GA)	3 mL L^{-1} (GA)	2 mL L^{-1} (GA)	1 mL L^{-1} (GA)				
	Enhancement efficiency	153 to 604%	131 to 892%	211 to 996%	130 to 1078%				
Gadobutrol (MRI)	Conc. of barite	10%							
Barite (CT)	Signal attenuation (HU)	1095 to 1197							
Resin	Conc. of gadobutrol	Resin alone	2 mL L^{-1}	3 mL L^{-1}					
Gadobutrol (MRI)	Enhancement efficiency	345%	673%	938%					
Nutritional	Conc. of iodine	Resin alone	20 mg L^{-1}						
iodine (CT)	Signal attenuation (HU)	65.7	363.8						
Resin	Conc. of gadobutrol	2 mL L^{-1}	3 mL L^{-1}						
Gadobutrol (MRI)	Enhancement efficiency	−14%	−8%						
Aluminium (CT)	Conc. of aluminum	7 g L^{-1}	14 g L^{-1}	20 g L^{-1}					
	Signal attenuation (HU)	44.7	57.5	66/5					

conc., concentration.

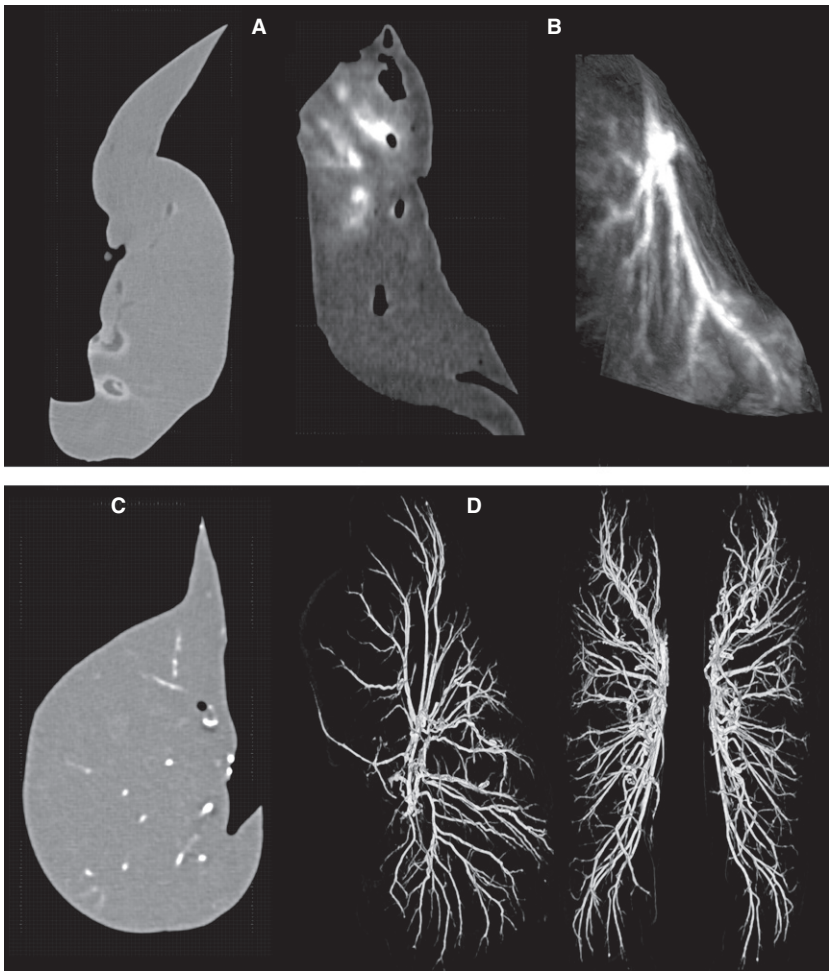

Fig. 1 CT results of pig liver arterial trees injected with (A,B) a mixture of iodine (30 mg mL^{-1}) and $CuSO_4$ or gadoxetic acid (A: planar images; B: 3D visualization), and (C,D) a mixture of barite (10%) and $CuSO_4$ or gadoxetic acid (C: planar images; D: 3D visualization).

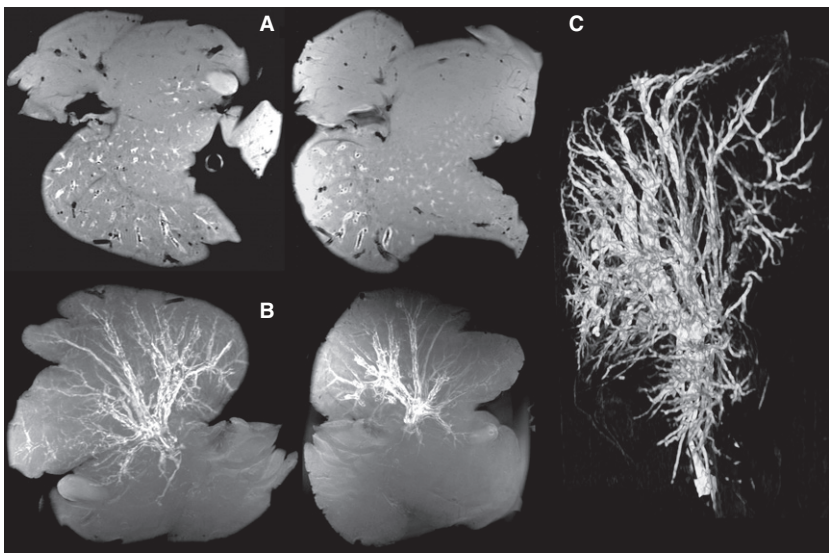

Fig. 2 MRI (A,B) and CT (C) results of pig liver arterial trees injected with a mixture of latex, gadobutrol and barite. (A: MRI planar images; B: MRI 3D visualization; C: CT 3D visualization).

Finally, following our *in vitro* results, we tested resin mixed with gadobutrol (3 mL L^{-1}) and either nutritional iodine (20 mg L^{-1}) or aluminum powder at a concentration of 100 g L^{-1}. The MRI results showed good contrast (enhancement efficiency 112%) when mixed with aluminum or nutritional iodine, with correct 3D reconstructions of the

© 2017 Anatomical Society

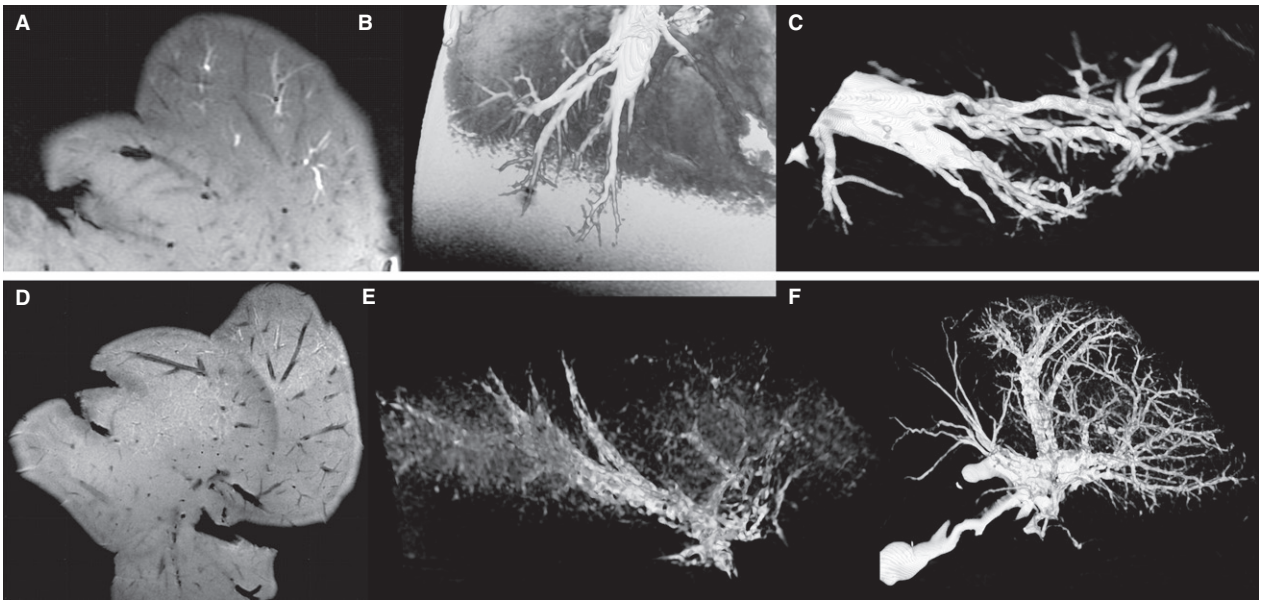

Fig. 3 MRI (A,B,D,E) and CT (C,F) results of pig liver arterial trees injected with agar–gadobutrol–barite (A–C) mixture and silicone–gadobutrol–barite (D–F) mixture. (A,D: MRI planar images; B,E: MRI 3D visualizations; C,F: CT 3D visualizations).

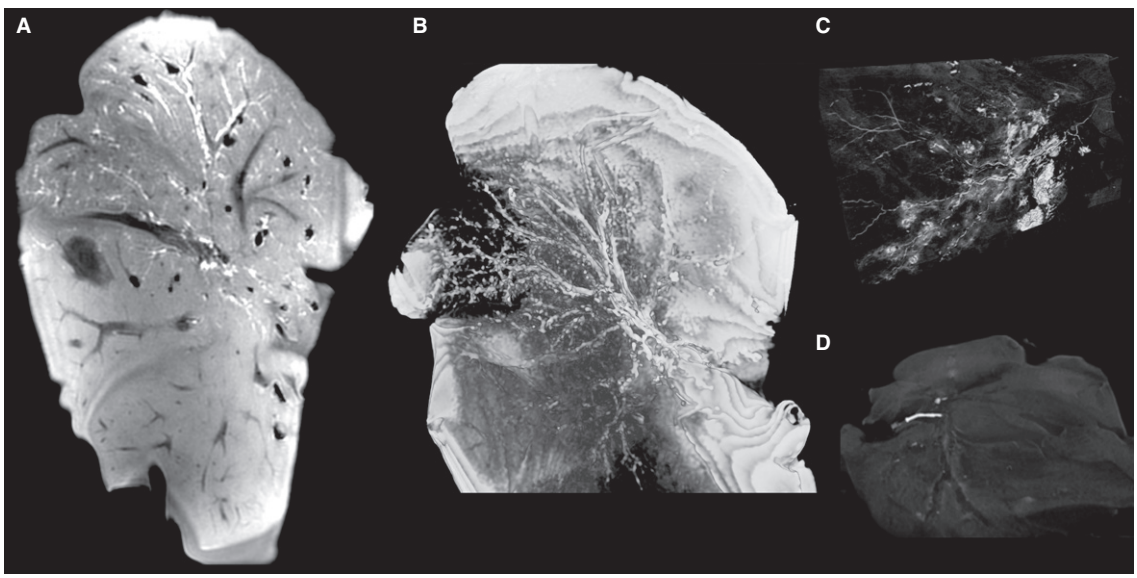

Fig. 4 MRI (A,B) and CT (C,D) results of pig liver arterial trees injected with a mixture of resin, gadobutrol (A,C) and aluminium (B) or nutritional iodine (D).

arterial trees (Fig. 4). Unfortunately, the mixtures of aluminum or nutritional iodine did not provide homogeneous or sufficient contrast at CT.

According to *in vitro* and *ex vivo* porcine results, the most interesting mixture is composed of colorized latex, gadobutrol and barite. The protocol allowed correct CT and MRI imaging, as well as accurate gross dissection (Fig. 5).

Discussion

In our work, all mixtures were first tested *in vitro* to adjust concentrations, and then tested on *ex vivo* pig livers and one human pancreas.

We chose pig liver because it provides an excellent model in anatomy and experimental surgery as it is technically simple to remove, easily obtainable and presents a similar

© 2017 Anatomical Society

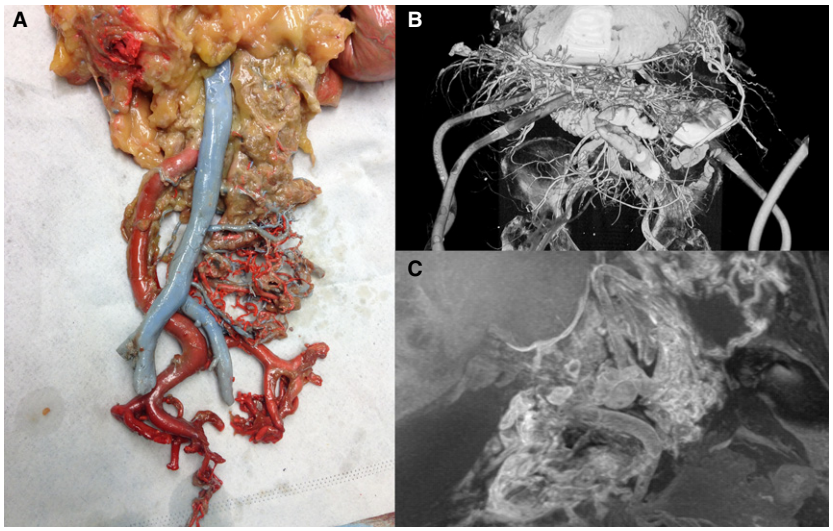

Fig. 5 (A) Dissection of the vessel tree (arteries in blue and veins in red) of a human pancreas. The mixture injected is composed of latex–gadobutrol–barite and was previously imaged both at CT(B) and MRI (C).

anatomy, physiology and size to human liver (Baulieux et al. 1972).

Cast products

In this study we tested the most common molding products, easily obtained in most stores for any anatomy laboratory. Leonardo da Vinci and Jakobus Berengius were the first in the beginning of the 16th century to realize wax cast of hollow anatomic structures (Grabherr et al. 2007). For vascular trees, this protocol implies injection of a suitable material into the vascular system, where it hardens. Various casting materials have been tested over the years, such as mixtures of lead, bismuth, cadmium, celluloid and celloidin. Nylon, neoprene latex and different resins were introduced later, in the beginning of the 20th century (Grabherr et al. 2007).

Latex is largely used for gross dissections (Stokes et al. 1998; Zenn & Heitmann, 2003) and as a suspending medium for various contrast agents, giving homogeneous mixtures (Stokes et al. 1998; Godat et al. 2004). Its fluidity facilitates and optimizes the injection, and results in deeper penetration, allowing excellent distribution in distal vessels (Bergeron et al. 2006; Alvernia et al. 2010). When colored with classical pigments, it can easily be identified during dissection. Its elasticity maintains the integrity of the vessels. Liquid latex contains about one-third latex and two-thirds water. As it dries, it solidifies to a rubbery consistency, in 15–20 min in very small vessels, but hours or even days in very large vessels. Ventilation and heating system may accelerate the setting of the latex.

Colored silicone is largely used in dissecting rooms (Sanan et al. 1999; Zhao et al. 2002). Silicone should be diluted up to 30% in our experience, because this component was of course not viscous enough to allow manual injection. Many producers sell fluids that will lower the viscosity of silicone rubber products. Unfortunately, tensile strength after hardening is reduced in proportion to the amount of diluents added. Once the hardener has been incorporated (5%), setting time varies from 20 to 30 min, allowing an injection without feverish haste. In our experience, as others (Grabherr et al. 2007; Alvernia et al. 2010), silicone injection is very tricky compared with latex injection.

Polyurethane resin is composed of two components: the resin and the hardener. It hardens very fast but it is easy to find resin that hardens in 30 min. It does not give off any odors and is safe to handle. Resin polyurethane is resistant against acids and can be used for the injection-corrosion technique (Meyer et al. 2007). In our experience, mixing the resin with iodine and barite produces an emulsion reaction, preventing its use for any injection.

Other teams reported their results using epoxy resin without emulsion reaction, but degassing. They underlined the toxicity of their experiments, necessitating specific, expensive equipment (Bulla et al. 2014; Kingston et al. 2016).

Gelatin and agar are largely used for injections because they are easy to obtain and to handle (Plaisant et al. 1998; Thomas et al. 2005; Mahato, 2016). Some teams consider this injection protocol a ‘gold standard’ (Bergeron et al. 2006). Gelatin can be mixed with all contrast agents such as lead oxide, lead phosphate, barium iodine, and gadolinium (Plaisant et al. 1998; Bergeron et al. 2006). This technique requires warming the mixture just before injection. Unfortunately, it hardens quickly, especially if the injected organs are cold.

Contrast agents

Current contrast agents can be categorized as corpuscular preparations, oily liquids, hydrosoluble solutions or casts (Grabherr et al. 2007). In the present study, we focused on casts (contrast agent in a suspending medium that hardens), since our aim was to be able to dissect vessel trees after imaging.

© 2017 Anatomical Society

In this study we tested the most known contrast agents for CT. Iodine is largely used in clinical practice as a radiopaque marker. The hydrosoluble solutions are easily injectable and essential for *in vivo* imaging (Liu et al. 2012). Nevertheless, traditional injectable iodine alone is rarely used in postmortem injection since it rapidly diffuses through vessel walls when dissolved in water, as we have shown, and contributes a relatively poor amount of radiopacity (Grabherr et al. 2007; Young et al. 2008). Lead oxide was considered the standard for blood vessel visualization, used by numerous teams (Rees & Taylor, 1986; Bergeron et al. 2006), habitually mixed in gelatin, latex or silicone. For example, Segerberg-Kottinen introduced the silicone rubber–lead oxide technique in 1987 (Segerberg-Konttinen, 1987), the most practiced method for microangiography. Nevertheless, because of its high toxicity, lead oxide requires special precautions to be handled and cannot be used routinely in laboratories without expensive, specific equipment (Quinodoz et al. 2002; Kingston et al. 2016). Some manufacturers have developed special casting materials for microangiography (Jorgensen et al. 1998; Djonov et al. 2000) but these are very expensive and not suitable for macro-organ injections. Barium sulfate is a well-known radiographic contrast agent, first described in 1920 (Bergeron et al. 2006). Typically water-soluble, it is generally mixed with gelatin or latex. Its ability to provide contrast is solvent-dependent (it enters capillaries when dissolved in water but not in gelatin) (Young et al. 2008). However, interest in this agent has gained renewed interest, as lead oxide cannot be routinely used any longer (Quinodoz et al. 2002; Kingston et al. 2016). Barium sulfate has recently been proved to be more accurate than lead oxide for high resolution micro-CTs and is preferred due to its non-toxicity (Blery et al. 2016; Kingston et al. 2016). Contrary to iodine, barium sulfate does not diffuse through vessels in postmortem studies.

MRI is the best tool for investigating organ parenchyma and soft tissues (Plaisant et al. 1998; Grabherr et al. 2015). The introduction of postmortem MRI studies for forensic investigations, compared with conventional autopsy, has brought great benefits, in particular MRI angiography (Grabherr et al. 2015). For these reasons, despite the difficulties of accessibility and the time needed for the imaging sequences, MRI studies on injected *ex vivo* organs should be part of anatomic work (Plaisant et al. 1998; Grabherr et al. 2007; Ruder et al. 2014). Nevertheless, the development of the best MRI contrast agent for postmortem or *ex vivo* studies remains a challenge (Bruguier et al. 2015; Grabherr et al. 2015).

Gelatin and agar, used alone or mixed with various contrast agents, are known as excellent markers for MRI (Schindel et al. 2013), as confirmed by our results. Nevertheless, vessel trees injected with gelatin or agar is too soft to dissect and will not give an accurate cast of vessel trees. Gadolinium is the most classical contrast agent for MRI studies and copper sulfate has been reported as an accurate MRI marker (Schindel et al. 2013). Nevertheless, alone or mixed with latex, resins or silicone, gadoxetic acid or copper sulfate can distribute to the extracellular space quickly and freely (Aime & Caravan, 2009). This extravasation, as reported in our study and by other teams, makes the use of these agent impossible, in particular in *ex vivo* studies (Grabherr et al. 2007).

Gadolinium mixed with gelatin is currently the injection medium of choice for MRI studies, since the rapid hardening of gelatin prevents extravasation of gadolinium (Plaisant et al. 1998). Nevertheless, without an radiopaque agent this mixture does not allow CT studies and the problem of the dissection using gelatin remains.

Gadobutrol (Gadovist®) is a non-ionic, macrocyclic gadolinium-based contrast agents with high T1-relaxivity (Michaely et al. 2017). The macrocyclic chemical structure contributes to the high kinetic stability of gadobutrol compared with linear contrast agents, and is associated with a lower propensity to release gadolinium ions (Prince et al. 2017). Gadobutrol is known to be less likely to diffuse throughout tissues and microvasculature (Helms et al. 2016). In our experience, gadobutrol is the best contrast agent for MRI for its stability in cadaveric vessels, but should be injected just before the imaging.

Several studies have reported different injection protocols and imaging parameters. In particular, oily contrast agent allows for high-contrast angiographic images in MRI studies since oily liquids are retained by vessels for longer periods without extravasation. Angiofil® (Fumedica, Muri, Switzerland) enabled detailed vascular assessment and revealed the utility oily contrast agent for postmortem MRI imaging, providing complete gross anatomic diagnoses similar to autopsy (Bruguier et al. 2015). However, this preparation does not harden, making it impossible to dissect after imaging. Moreover, it is not miscible with CT contrast agents and its ability to penetrate the microcirculation is viscosity-dependent (Grabherr et al. 2007; Young et al. 2008).

To the best of our knowledge, none of the *ex vivo* studies defined what a 'good' contrast should be, or proved scientifically the capacity of the cast to distribute to very distal vessels.

Difficulties encountered with injections

Injections with latex were simple, easy to perform with very reproducible results. Nevertheless, the hardening of the product might be time-consuming for the largest vessels or cavities. Agar needed to be boiled before mixed with contrast agent, and should be injected at a temperature below 50 °C to avoid burning the injected vessels. As a consequence, it hardened fast in cold *ex vivo* organs and distal small vessels were not always filled with contrast agents. Furthermore, solidified agar remained fragile and dissection of small vessels was not possible. Nevertheless, agar is very

© 2017 Anatomical Society

simple to produce and to inject. Silicone should be extremely diluted, with more than 30% of diluents in our experience (although manufacturers usually recommended 10% maximum). As a consequence, it was not hard enough to allow correct castings. In spite of the dilution, injection with silicone was difficult because it was not fluid enough and the injection could not be monitored correctly. Injection of resin was not very difficult since we used a polyurethane resin which hardened slowly. Nevertheless, the mixture remained relatively viscous, probably due to the gadobutrol, aluminum or nutritional iodine. The high injection pressure, as for silicon, and the necessity of mixing the different chemical components for a long time, led sometimes to inhomogeneous contrast, artifacts and occasionally the formation of bubbles (Figs 3E and 4A,C), as reported by other authors (Jackowski et al. 2008; Grabherr et al. 2014).

Recommendations

As far as we know, this is the first report of a study comparing the most popular products for *ex vivo* injection, that allowing contrast enhancement both for CT and MR imaging studies and that harden to allow gross dissection of the vessel trees or anatomic cavities. This injection protocol allows comparative anatomical analysis of the vascularization of cadaveric specimens. Some authors have reported their techniques of injecting a contrast agent and casting product material for CT studies following by dissection (Bergeron et al. 2006; Bulla et al. 2014) or combining MRI and CT contrast agents but without dissection (Plaisant et al. 1998; Grabherr et al. 2007).

The aim of our study was to take stock of the current techniques for *ex vivo* injections. We selected the mixtures that allowed both computed tomography and magnetic resonance imaging studies on the same anatomic specimen, and that were able to harden for gross dissection.

Our results allow us to provide the best protocols for *ex vivo* anatomic studies:

1 For *ex vivo* MRI study without gross dissection, oily contrast agent should be used, such as Angiofil® (Bruguier et al. 2015) or any oily agent. For *ex vivo* CT study without gross dissection, a mixture of agar or gelatin and barite should be used, since it is easy to inject although difficult to dissect.
2 For *ex vivo* study combining MRI and CT without gross dissection, a mixture of agar or gelatin, gadobutrol and barite should be used. The injection can be performed hours before imaging.
3 For *ex vivo* study combining CT and MRI imaging and gross dissection, a mixture of colorized latex, gadobutrol and barite should be used and injected just before imaging.

To conclude, the development of imaging techniques has made it possible to observe anatomical structures in much greater detail. The help of computer technology and post-processing software allows easy 3D reconstruction of complex anatomical structures.

Author contributions

Y. Renard, G. Hossu and B. Chen contributed to concept/design. Y. Renard, G. Hossu and M. Krebs performed the acquisition of data. Y. Renard, G. Hossu, M. Labrousse and M. Perez contributed to data analysis/interpretation. Y. Renard, G. Hossu and B. Chen realized the drafting of the manuscript. G. Hossu, B. Chen, M. Labrousse and M. Perez made the critical revision of the manuscript and approved the article.

Conflict of interest

The authors have no conflict of interest to declare.

References

Aime S, Caravan P (2009) Biodistribution of gadolinium-based contrast agents, including gadolinium deposition. *J Magn Reson Imaging* **30**, 1259–1267. https://doi.org/10.1002/jmri.21969.

Alvernia JE, Pradilla G, Mertens P, et al. (2010) Latex injection of cadaver heads: technical note. *Neurosurgery* 67,362–367.

Baulieux J, Berard P, Cret R, et al. (1972) The anatomy of pig-liver (*Sus scrofa domesticus*) (author's translation). *Arch Anat Histol Embryol Norm Exp* **55**, 209–231.

Bergeron L, Tang M, Morris SF (2006) A review of vascular injection techniques for the study of perforator flaps. *Plast Reconstr Surg* **117**, 2050–2057.

Blery P, Pilet P, Bossche AV, et al. (2016) Vascular imaging with contrast agent in hard and soft tissues using microcomputed-tomography. *J Microsc* **262**, 40–49.

Bruguier C, Egger C, Vallée JP, et al. (2015) Postmortem magnetic resonance imaging of the heart *ex situ*: development of technical protocols. *Int J Legal Med* **129**, 559–567.

Bulla A, Casoli C, Farace F, et al. (2014) A new contrast agent for radiological and dissection studies of the arterial network of anatomic specimens. *Surg Radiol Anat* **36**, 79–83.

Djonov V, Schmid M, Tschanz SA, et al. (2000) Intussusceptive angiogenesis: its role in embryonic vascular network formation. *Circ Res* **86**, 286–292.

Friedl R, Preisack MB, Klas W, et al. (2002) Virtual reality and 3D visualizations in heart surgery education. *Heart Surg Forum* **5**, E17–E21.

Fye WB (1984) Coronary arteriography – it took a long time! *Circulation* **70**, 781–787.

Godat DM, Sanger JR, Lifchez SD, et al. (2004) Detailed neurovascular anatomy of the serratus anterior muscle: implications for a functional muscle flap with multiple independent force vectors. *Plast Reconstr Surg* **114**, 21–29.

Grabherr S, Djonov V, Yen K, et al. (2007) Postmortem angiography: review of former and current methods. *Am J Roentgenol* **188**, 832–838.

Grabherr S, Grimm J, Dominguez A, et al. (2014) Advances in post-mortem CT-angiography. *Br J Radiol* **87**, 20130488.

© 2017 Anatomical Society

Grabherr S, Grimm J, Baumann P, et al. (2015) Application of contrast media in post-mortem imaging (CT and MRI). *Radiol Med (Torino)* **120**, 824–834.

Helms G, Schlumbohm C, Garea-Rodriguez E, et al. (2016) Pharmacokinetics of the MRI contrast agent gadobutrol in common marmoset monkeys (*Callithrix jacchus*). *J Med Primatol* **45**, 290–296.

Hylton N (2006) Dynamic contrast-enhanced magnetic resonance imaging as an imaging biomarker. *J Clin Oncol* **24**, 3293–3298.

Jackowski C, Persson A, Thali MJ (2008) Whole body postmortem angiography with a high viscosity contrast agent solution using poly ethylene glycol as contrast agent dissolver. *J Forensic Sci* **53**, 465–468.

Jorgensen SM, Demirkaya O, Ritman EL (1998) Three-dimensional imaging of vasculature and parenchyma in intact rodent organs with X-ray micro-CT. *Am J Physiol* **275**, H1103–H1114.

Kamali P, Dean D, Skoracki R, et al. (2016) The current role of three-dimensional printing in plastic surgery. *Plast Reconstr Surg* **137**, 1045–1055.

Kingston MJ, Perriman DM, Neeman T, et al. (2016) Contrast agent comparison for three-dimensional micro-CT angiography: a cadaveric study. *Contrast Media Mol Imaging* **11**, 319–324.

Lange T, Indelicato DJ, Rosen JM (2000) Virtual reality in surgical training. *Surg Oncol Clin N Am* **9**, 61–79 vii.

Liu Y, Ai K, Lu L (2012) Nanoparticulate x-ray computed tomography contrast agents: from design validation to *in vivo* applications. *Acc Chem Res* **45**, 1817–1827.

Mahato NK (2016) Implications of structural variations in the human sacrum: why is an anatomical classification crucial? *Surg Radiol Anat* **38**, 947–954.

Meyer EP, Beer GM, Lang A, et al. (2007) Polyurethane elastomer: a new material for the visualization of cadaveric blood vessels. *Clin Anat* **20**, 448–454.

Michaely HJ, Aschauer M, Deutschmann H, et al. (2017) Gadobutrol in renally impaired patients: Results of the GRIP Study. *Invest Radiol* **52**, 55–60.

Nikolaou K, Becker CR, Muders M, et al. (2004a) Multidetector-row computed tomography and magnetic resonance imaging of atherosclerotic lesions in human *ex vivo* coronary arteries. *Atherosclerosis* **174**, 243–252.

Nikolaou K, Becker CR, Flohr T, et al. (2004b) Optimization of *ex vivo* CT- and MR- imaging of atherosclerotic vessel wall changes. *Int J Cardiovasc Imaging* **20**, 327–334.

Pabst AM, Ackermann M, Wagner W, et al. (2014) Imaging angiogenesis: Perspectives and opportunities in tumour research – A method display. *J Cranio-Maxillofac Surg* **42**, 915–923.

Pauwels R, Silkosessak O, Jacobs R, et al. (2014) A pragmatic approach to determine the optimal kVp in cone beam CT: balancing contrast-to-noise ratio and radiation dose. *Dentomaxillofacial Radiol* **43**, 20140059.

Plaisant O, Sarrazin JL, Gillot C, et al. (1998) Technique for injection of the lumbar vertebral venous plexuses employed in anatomic, computed tomography and magnetic resonance imaging studies. *Surg Radiol Anat* **20**, 113–118.

Prince MR, Lee HG, Lee C-H, et al. (2017) Safety of gadobutrol in over 23,000 patients: the GARDIAN study, a global multicentre, prospective, non-interventional study. *Eur Radiol* **27**, 286–295.

Pujol S, Baldwin M, Nassiri J, et al. (2016) Using 3D modeling techniques to enhance teaching of difficult anatomical concepts. *Acad Radiol* **23**, 507–516.

Quinodoz P, Quinodoz M, Nussbaum J-L, et al. (2002) Barium sulphate and soft-tissue radiology: allying the old and the new for the investigation of animal cutaneous microcirculation. *Br J Plast Surg* **55**, 664–667.

Rees MJ, Taylor GI (1986) A simplified lead oxide cadaver injection technique. *Plast Reconstr Surg* **77**, 141–145.

Ruder TD, Thali MJ, Hatch GM (2014) Essentials of forensic postmortem MR imaging in adults. *Br J Radiol* **87**, 20130567.

Sanan A, Abdel Aziz KM, Janjua RM, et al. (1999) Colored silicone injection for use in neurosurgical dissections: anatomic technical note. *Neurosurgery* **45**, 1267–1271; discussion 1271–1274.

Saran U, Gemini Piperni S, Chatterjee S (2014) Role of angiogenesis in bone repair. *Arch Biochem Biophys* **561**, 109–117.

Schindel J, Muruganandham M, Pigge FC, et al. (2013) Magnetic resonance imaging (MRI) markers for MRI-guided high-dose-rate brachytherapy: novel marker-flange for cervical cancer and marker catheters for prostate cancer. *Int J Radiat Oncol Biol Phys* **86**, 387–393.

Segerberg-Konttinen M (1987) Demonstration of esophageal varices postmortem by gastroesophageal phlebography. *J Forensic Sci* **32**, 703–710.

Stokes RB, Whetzel TP, Sommerhaug E, et al. (1998) Arterial vascular anatomy of the umbilicus. *Plast Reconstr Surg* **102**, 761–764.

Thomas BP, Geddes CR, Tang M, et al. (2005) The vascular basis of the thoracodorsal artery perforator flap. *Plast Reconstr Surg* **116**, 818–822.

Xiao J, Cui Z, Fu M, et al. (2016) An ex vivo liver training model continuously perfused to simulate bleeding for suture skills involved in laparoscopic liver resection: development and validity. *Surg Endosc* **30**, 4553–4561.

Young S, Kretlow JD, Nguyen C, et al. (2008) Microcomputed tomography characterization of neovascularization in bone tissue engineering applications. *Tissue Eng Part B Rev* **14**, 295–306. https://doi.org/10.1089/ten.teb.2008.0153.

Zenn MR, Heitmann C (2003) Extended TRAM flap: feasibility study on fresh human cadavers. *Ann Plast Surg* **50**, 256–262.

Zhang Y-Z, Li Y-B, Tang M-L, et al. (2007) Application of three-dimensional digitalized reconstruction of an anterolateral thigh flap and an arterial dorsalis pedis flap. *Microsurgery* **27**, 553–559.

Zhao J, Chen C, Rosenblatt SS, et al. (2002) Imaging the cerebrovascular tree in the cadaveric head for planning surgical strategy. *Neurosurgery* **51**, 1222–1227; discussion 1227–1228.

© 2017 Anatomical Society